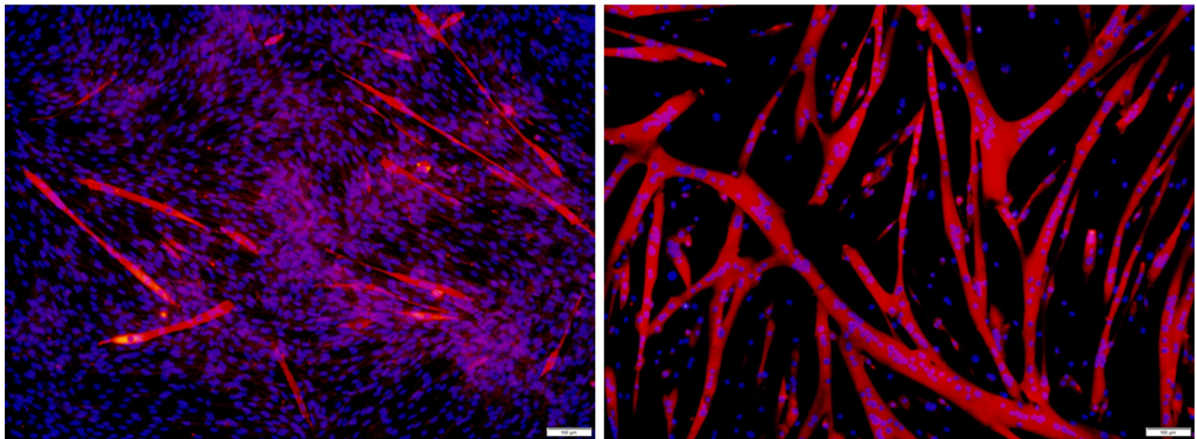


Supplement Figure 1: Cultured primary satellite cells and C2C12 myotubes

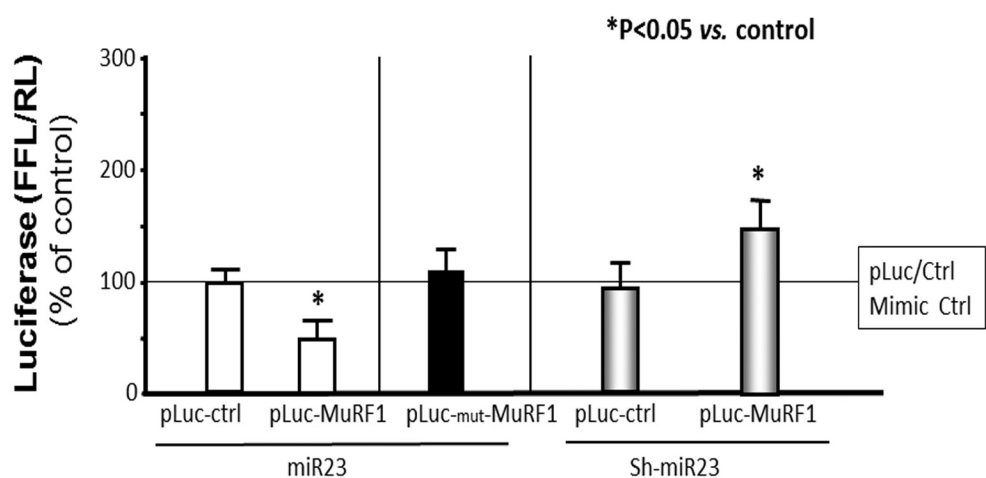


C2C12 cells
in 2% HS with DMEM medium

satellite cells
in 20% FBS with F-10 medium

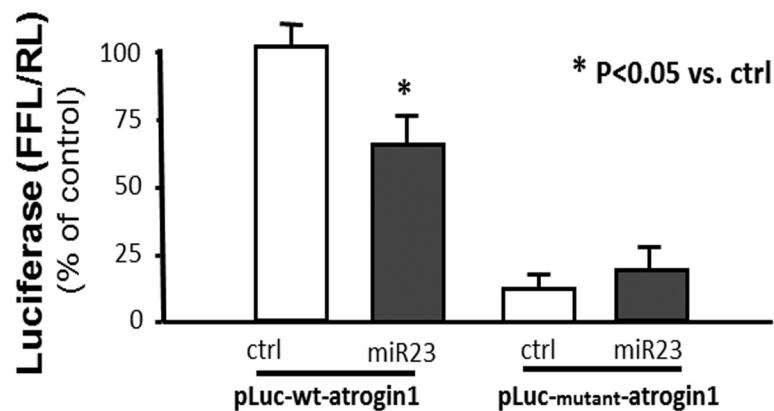
Supplement Figure 1: Cultured primary satellite cells and C2C12 myotubes: To evaluate the differentiation status of myotubes, embryonic myosin heavy chain (eMyHC, a marker of myotube formation) was detected immunohistochemically in C2C12 cells (Left, fifth passage) and primary satellite cells (Right, third passage). Both sets of cells were differentiated for 2 days. eMyHC is indicated by red staining; DAPI (blue) staining was used to detect nuclei.

Supplement Figure 2: miR-23a binds to the 3'-UTR of TRIM63/MuRF1



Supplement Figure 2: miR-23a binds to the 3'-UTR of TRIM63/MuRF1. Satellite cells were transfected with pMIR-REPORT Luciferase (indicated as pLuc-ctrl), pMIR-wt-MuRF1 or pMIR-mutant-MuRF1 and incubated with either a miR-23a mimic (miR23) or miR-23a-inhibitor (Sh-miR23); a control Renilla luciferase plasmid was included to normalize firefly luciferase activity. The mean normalized luciferase activity in cells transfected with the control plasmid and incubated with a scrambled control miR mimic was designated as the 100% reference activity (designated by a horizontal line in the graph). The other bars show the response of the cells to miR-23a mimic or sh-miR23a expressed as a percent of the control level for each experiment. Each treatment was measured in triplicate wells and each experiment was repeated three times; the results were combined to calculate differences between treatment groups. Data are reported as the mean \pm s.e. percentage of the normalized control luciferase activity (n=9; *p<0.05 vs. control miR).

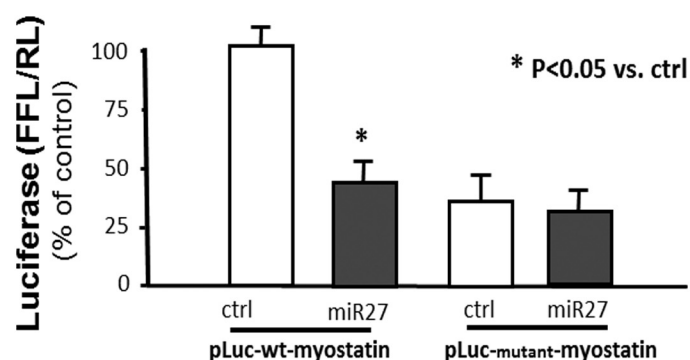
Supplement Figure 3: miR-23a binds to the 3'-UTR of FBXO32/atrogin-1



Supplement Figure 3: miR-23a binds to the 3'-UTR of FBXO32/atrogin-1.

Satellite cells were transfected with pLuc-wt-atrogin1 and pLuc-mutant-atrogin1 with miR23 mimic (miR23) or mimic control (ctrl). Bars in the graph indicate the response of cells to miR-23a or a control miR, expressed as a percent of the control level (pLuc-wt-atrogin1 plus control miR) for each treatment. Each treatment was measured in triplicate wells and each experiment was repeated three times; the results were combined to calculate differences between treatment groups. Data are reported as the mean \pm s.e. percentage of the normalized control luciferase activity (n=9; *p<0.05 vs. control miR).

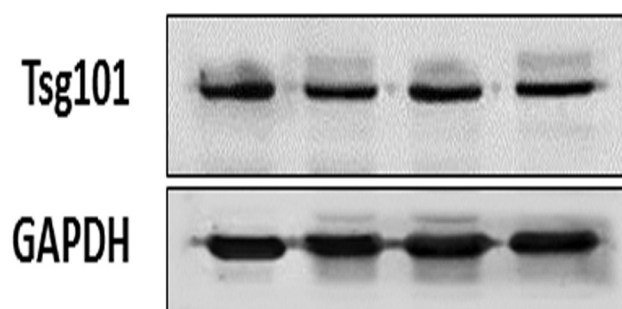
Supplement Figure 4: miR-27a binds to the 3'-UTR of myostatin.



Supplement Figure 4: miR-27a binds to the 3'-UTR of myostatin.

Satellite cells were transfected with constructs containing the miR-27a binding site in the myostatin 3'-UTR (pLU-wt-myostatin) or mutated miR-27a binding site (pLU-mutant-myostatin) and incubated with a control miR or miR-27a mimic (miR27). Bars in the graph indicate the response of cells to miR-27a or a control miR, expressed as a percent of the control level (pLuc-wt-atrogin1 plus control miR) for each treatment. Each treatment was measured in triplicate wells and each experiment was repeated three times; the results were combined to calculate differences between treatment groups. Data are reported as the mean \pm s.e. percentage of the normalized control luciferase activity (n=9; *p<0.05 vs. control miR).

Supplement Figure 5: Protein abundance in serum exosomes from sham and CKD mice



Supplement Figure 5: Protein abundance in serum exosomes from sham and CKD mice.

The exosomal protein TSG101 and Glyceraldehyde 3-phosphate dehydrogenase (GAPDH) were evaluated by western blot analysis of serum-derived exosomes from control and CKD mice. No difference in protein content was found among cohorts.

Supplement Methods:

Animals and CKD model: The CKD animal model and adeno-associated virus muscle injection experiments were approved by the institutional animal care and use committee of Emory University. CKD was induced in a two-step process¹. First, the right kidney was removed from anesthetized mice (xylazine 12 mg/kg, ketamine 60 mg/kg). One week later, two poles of the left kidney (second surgery) were removed; hemostasis was achieved by cautery and pressure. After the second surgery, the sham and CKD mice were fed a low protein diet (Harlan Teklad: 14% protein, 3.5% fat, 49% carbohydrate) with 0.45% NaCl added to their drinking water for 1 week. Then, the mice were fed a high-protein diet (40% protein) for 3 additional weeks. Starting with the low protein diet, a modified pair-feeding protocol was used in which the amount of food consumed by each CKD mouse was provided to a matched mouse in each of the other three cohorts. Blood urine nitrogen (BUN) was measured using a BUN Kinetic Procedure Kit (Thermo Electron, Louisville, CO.).

Muscle function was measured using a mouse grip strength meter with dual computerized sensors to detect and record the grip force (Columbus Instruments, Columbus, OH). Mice are allowed to grip a grid net that connected to a force transducer and gently pulled by the tail for 5 seconds. The computerized sensors determine what force was needed to counter-balance the grip of the mice. Mice were tested before the CKD surgery to make sure that all group mice have similar grip strength (data not shown), and before harvesting the muscle. The grip strength of each mouse was tested 5 times on each testing occasion, with 10 minutes rest between each test. The average of the 5 determinations was reported¹.

Production of high titer adeno-associated virus (AAV): The miR-23a/27a/24-2 gene cluster was cloned into the AAV vector pTR.UF5 (pTR.UF5.miR-23a/27a/24-2) by Emory Integrated Genomics Core. The AAV was produced using three plasmids system and qPCR was used for titer by the Emory Viral Vector Core. The stock virus titer was 3.4×10^{14} viral genome/ml (vg/ml) for AAV-miR-23/27/24-2 and 6.5×10^{14} vg/ml AAV-GFP. For in vivo AAV transduction, 20 μ l of diluted virus (10^{10} vg) was injected into the tibialis anterior (TA) muscle of anesthetized mice over 5-7 min using a Hamilton syringe with a 30 gauge needle. One min after cessation of the injection, the needle

was retracted 1 mm and then left in place for an additional one min before being slowly withdrawn from the muscle. Each injection took ~10 min. Both legs of the mouse were injected with the same type and same amount of AAV.

Caspase-3 and -7 activity: Gastrocnemius muscle was pulverized under liquid nitrogen and homogenized in lysis buffer (100 mM N-[2-hydroxyethyl] piperazine-N-[2-ethanesulphonic acid], 10% sucrose, 0.1%, NP-40 and anti-protease cocktail 1 tablet / 10 ml (Roche 1836153), pH 7.4). The protein content of supernatants was quantified with the DC Protein Assay kit (Bio-Rad, Hercules, CA, USA). We measured the activity of specific caspases using a fluorogenic substrate (Ac-DEVD-7-amino-4-methylcoumarin (AMC) for both caspase-3 and -7 CaspACE Assay System (Promega Madison, WI) with and without a caspase-3 inhibitor (Ac-DEVD-CHO) or caspase- 7 inhibitor (Ac-DQTD-CHO). Fluorescence was measured in a fluorometer (Shimadzu) with a 380 nm excitation wavelength and a 460 nm emission wavelength. The difference between the substrate cleavage activity levels in the presence and absence of caspase inhibitor was used to calculate the contribution of caspase-3 and -7 activities².

Western Blot and antibodies: Hind limb muscle were homogenized in a lysis buffer (10 mM Tris-HCl, 10 mM NaCl, 2 mM EDTA, 0.5 % NP-40, 1 % glycerol, containing 1 mM Na₃VO₄; 10µg/ml PMSF; 5µg/ml aprotinin; 1µg/ml leupeptin plus phosphatase inhibitors cocktails 1 and 2 (Sigma). Protein concentrations were measured using a RC-PC protein assay kit (Bio-Rad). Equal amounts of protein (10-30 µg) samples were separated in denaturing polyacrylamide gels, transferred to a PVDF membrane which was blocked and incubated with specific primary antibodies^{3, 4}. Primary antibodies included Akt/p-Akt (Ser473), FoxO1/p-FoxO1 (Thr32), FoxO3/p-FoxO3 (Thr32), pSmad2/3 (D27F2) and Smad2/3 (D7G7) from Cell Signaling; MyoD, myogenin, and eMyHC antibodies were from DSHB (University of Iowa, Iowa, IA). pTEN (FL-403) antibody was from Santa Cruz (Santa Cruz, CA); GAPDH antibody was from Millipore (Burlington, MA); myostatin antibody was from Abcam (Cambridge, MA); YY1 antibody was from Santa Cruz (Santa Cruz, CA). Secondary antibodies used included Alexa Fluor® 680 goat anti-Rabbit IgG or goat anti-mouse IgG from Invitrogen (Carlsbad, CA). Protein bands were scanned and quantified using a Li-cor Odyssey

infrared scanning system (Li-COR Biosciences, Lincoln, Nebraska). To assess myofibrillar protein degradation, the level of the 14-kDa actin biomarker fragment in frozen muscles was measured. Muscles were harvested and homogenized in hypotonic buffer (0.5 M HEPES-KOH (pH7.5); 10 mM MgCl₂; 1 mM EDTA; 1 mM EGTA and fresh added: 1 mM Na₃VO₄; 10 µg/ml PMSF; 5 µg/ml aprotinin; 1 µg/ml leupeptin) with phosphatase inhibitors cocktail 1 and 2 (Sigma). The pellet fraction of the muscle homogenate was solubilized in 2X Laemmli sample buffer and boiled for 10 min. The 14-kD actin fragment were detected by standard western blotting as described above using poly-clonal antibodies against the C-terminal 11 amino acids of actin (1:500 dilution, Sigma-Aldrich, St. Louis, MO).

Primary muscle satellite and C2C12 cell culture: Satellite cells were isolated from hind-limb muscles of 4 month old mice. Dissociation of mouse skeletal muscle tissue into single-cell suspensions was performed using a Skeletal Muscle Dissociation Kit (130-098-305; MACS, Miltenyi Biotec, Inc. Auburn, CA) and a Satellite Cell Isolation Kit (130-104-267, MACS) was used to isolate muscle satellite cells. The isolated cells were cultured in Ham's F-10 Nutrient Mixture medium (Invitrogen) with 20% fetal bovine serum (FBS), 100 u/ml penicillin, 100 µg/ml streptomycin. Medium supplemented with 5 ng/ml human β -fibroblast growth factor (Atlanta Biologicals, Atlanta, GA) to inhibit cells differentiation; β -fibroblast growth factor was removed to induce myoblasts differentiation into myotubes. Immunohistology was used to assess the purity of the culture. Satellite cells were identified using anti-eMYHC (supplement 1) while anti- α -smooth muscle actin (Sigma) was used to identify contaminating fibroblasts; no fibroblasts were detected (data not shown). Satellite cells were not used beyond passages 5.

C2C12 myoblasts are cultured in high glucose DMEM plus 10% FBS and antibiotics⁵. To differentiate the cells into myotubes, the growth medium was switched to high glucose DMEM plus 2% horse serum and antibiotics for 2-3 days. Passage more than 11 will be ended. C2C12 cells were not used beyond passages 10.

Luciferase reporter assay and transfection: For transfection, primary culture satellite cells were plated in growth media in 12-well plates. Each well of cells was incubated with 0.3 µg firefly luciferase reporter vectors and 0.08 µg of the Renilla

luciferase (transfection control vector) plus 200 nM microRNA mimic or control mimic (Dharmacon, Chicago, IL) along with Effectene transfection reagent (Qiagen, Valencia, CA). After 48 hours, firefly and renilla luciferase activities were measured by dual-luciferase assays (Promega). Luciferase activity was calculated as the ratio of firefly luciferase to renilla luciferase ($\times 100$)⁶. The pMIR-REPORT Luciferase Reporter plasmid was purchased from Applied Biosystems (Waltham, MA) and various targeting 3'-UTR constructs were made by the Emory University Integrated Genomics Core lab.

Exosome isolation: Serum was diluted with 5X PBS and organelles were eliminated by centrifugation at 1,000 x g for 10 min, 4°C. The supernatant fractions were further centrifuged at 16,000 x g for 30 min. The pellet from this step contains microparticles. The second supernatant was filtered through a 0.22 µm filter. Exosomes were pelleted by centrifugation at 120,000 x g for 90 min at 4°C (L8-70M ultracentrifuge, Beckman-Coulter, Indianapolis IN) and re-suspended in 100-400 µl PBS. Exosome protein was quantitated by a Bradford protein assay and the exosomal proteins marker, Tsg101, was evaluated by Western blot (Supplement Figure 5). Exosomal RNA was isolated using a miRNAeasy Kit (Qiagen Sciences, Germantown, MD) and quantified using NanoDrop spectrophotometry (Thermo Scientific, Wilmington, DE).

Reverse transcription and quantitative PCR (qPCR): Total RNA was extracted using Tri-Reagent (Molecular Research Inc., Cincinnati, OH). RNA concentrations were measured by spectrophotometry (Nano Drop Lite, Thermo Scientific, Wilmington, DE). To remove contaminating DNA, samples were treated with recombinant RNase-free DNase I (Thermo Fisher Scientific, West Palm Beach, FL). RNA was reverse transcribed to cDNA using the M-MLV Reverse Transcriptase (Invitrogen). Real-time qPCR was performed on CFX Connect™ Real-Time PCR Detection System (Bio-Rad, Hercules, CA) using SsoAdvUniver SYBR GRN SMX (Bio-Rad). The following cycle parameters were used: 94°C for 2 minutes and 40 cycles at 94°C for 15 seconds, 55°C for 30 seconds with final extension at 72°C for 10 minutes. Melting curve analysis was routinely performed to verify the specificity of the reaction. Primers (Table 2) were designed to cross intron-exon boundaries and generate amplicons in their linear ranges. For microRNA, the miR-CURY LNA™ Universal cDNA Synthesis kit (Exiqon, Woburn,

MA) was used for reverse transcription of RNA. The primers were custom designed by Exiqon. The miR-CUTY LNA microRNA PCR SYBR Green master mix (Exiqon) was used for qPCR with the following cycle parameters: 95°C for 10 minutes and 45 cycles at 95°C for 10 seconds and 60°C for 60 seconds. Expression of individual miRNAs were normalized using mouse U6 snRNA for microRNAs, miR-103a for exosomal microRNAs, and 18S rRNA for mRNAs. Differences between treatments were calculated using the $\Delta\Delta C_t$ method⁷.

Statistical analysis: Data were presented as mean \pm s.e. To identify significant differences between two cohorts, data were analyzed using a t-test. For comparison of more than two cohorts, a one-way ANOVA was performed; a post hoc Student-Newman-Keuls test was performed to identify differences between cohorts. In all cases, P values <0.05 were considered significant.

Disclosure

All the authors declared no competing interests.

1. Hu, L, Klein, JD, Hassounah, F, Cai, H, Zhang, C, Xu, P, Wang, XH: Low-Frequency Electrical Stimulation Attenuates Muscle Atrophy in CKD-A Potential Treatment Strategy. *J Am Soc Nephrol*, 26: 626-635, 2015.
2. Wang, XH, Hu, J, Du, J, Klein, JD: X-chromosome linked inhibitor of apoptosis protein inhibits muscle proteolysis in insulin-deficient mice. *Gene Ther*, 14: 711-720, 2007.
3. Zhou, Q, Du, J, Hu, Z, Walsh, K, Wang, XH: Evidence for adipose-muscle cross talk: opposing regulation of muscle proteolysis by adiponectin and Fatty acids. *Endocrinology*, 148: 5696-5705, 2007.
4. Su, Z, Robinson, A, Hu, L, Klein, JD, Hassounah, F, Li, M, Wang, H, Cai, H, Wang, XH: Acupuncture plus Low-Frequency Electrical Stimulation (Acu-LFES) Attenuates Diabetic Myopathy by Enhancing Muscle Regeneration. *PLoS One*, 10: e0134511, 2015.
5. Wang, XH, Zhang, L, Mitch, WE, LeDoux, JM, Hu, J, Du, J: Caspase-3 cleaves specific 19 S proteasome subunits in skeletal muscle stimulating proteasome activity. *J Biol Chem*, 285: 21249-21257, 2010.
6. Wang, XH, Hu, Z, Klein, JD, Zhang, L, Fang, F, Mitch, WE: Decreased miR-29 suppresses myogenesis in CKD. *J Am Soc Nephrol*, 22: 2068-2076, 2011.
7. Hu, Z, Klein, JD, Mitch, WE, Zhang, L, Martinez, I, Wang, XH: MicroRNA-29 induces cellular senescence in aging muscle through multiple signaling pathways. *Aging (Albany NY)*, 6: 160-175, 2014.